Monovacancy diffusion on Ag(100), Cu(100), and Ni(100): Prefactors and activation barriers

Ulrike Kürpick and Talat S. Rahman
Department of Physics, Cardwell Hall 116, Kansas State University, Manhattan, Kansas 66506
(Received 2 October 1998)

Our calculated activation barriers and preexponential factors show that monovacancy diffusion is an important constituent of mass transport on Ag(100), Cu(100), and Ni(100) and competes well with adatom diffusion. The contribution of lattice vibrations to the temperature dependence of the diffusion coefficient is incorporated through activation functions calculated in the harmonic approximation, invoking transition state theory and many-body interaction potentials from the embedded-atom method. On all three surfaces activation barriers are found to increase with the inclusion of lattice thermal expansion. [S0163-1829(99)01016-4]

I. INTRODUCTION

Diffusion on metal surfaces remains a subject of considerable interest because of its inherent relevance to thermally activated processes. On the one hand, a fundamental understanding of atomistic processes responsible for surface diffusion is necessary as it uncovers the nature of the temperature-dependent potential-energy surface experienced by the diffusing entity. On the other hand, diffusion plays a crucial role in many technologically important processes like thin-film and crystal growth, catalysis, and chemical reactions. Recent technical advances in several experimental techniques like scanning tunneling microscopy, He atom-surface scattering, and field ion microscopy, coupled with easy access to enhanced computational power and calculational methods, have led to a surge of activity in studies of surface diffusion. As precursors to developing an understanding of complex and technologically important systems, these works have concentrated on examination of the diffusion of adatoms, atomic clusters, and vacancy islands. In contrast to many studies of bulk- and grain-boundary diffusion in which the mobility of vacancies plays a central role,[1] the issue of monovacancy migration has remained on the sidelines because of the lack of definitive experimental evidence in its favor. This is not surprising since in growth processes, particularly at low temperatures, the density of vacancies on surfaces may not be significantly high to compete with deposited adatoms for mass transport. If vacancies do exist, the question naturally raised is the following: for what systems, and under what conditions, is the mobility of monovacancies a serious contender for surface self-diffusion? For the low Miller index surfaces of Ag, Cu, and Ni, several theoretical studies have addressed this issue partially.[2–9] Adatom diffusion appears to be favored over monovacancy's on Ni(100), Ni(111), and Ni(110),[4] and on Cu(111) and Cu(110),[5–7] while vacancy diffusion is predicted to dominate on Cu(100) (Ref. 3) and Ag(100).[8] Recently, an experimental study has also hailed migration of monovacancies as the most likely source of Ostwald ripening of homoepitaxially grown two-dimensional islands on Cu(100).[10] Hannon *et al.* explain the increasing growth of larger-sized clusters at the expense of the smaller ones by assuming mass transport between islands via the diffusion of vacancies instead of adatoms.

These results have been informative and, at least in the case of Cu(100), both pair potentials[5–7] and many-body potentials[3] arrive at the same conclusion. However, apart from the case of Cu(100) for which molecular-dynamics simulations have been used to obtain the diffusion coefficient,[9] these studies do not take into account the dynamical contributions to the diffusion coefficients. Instead, they focus on the energetics, i.e., the calculation of activation barriers at 0 K, which is the first step in any calculation. The other, and more challenging, step is the evaluation of the preexponential factor (''prefactor'' for simplicity) in the diffusion coefficient that depends also on the dynamical aspects of the potential energy surface. The tendency in molecular-dynamics simulations, as in experiments, is to extract numerical values for both the prefactor and the activation barrier from an Arrhenius plot. Since the origin of activation barriers is easier to comprehend and their magnitude may be obtained from other considerations, it is the prefactor that remains largely a fitting parameter, rather than an entity with physical significance.

To understand the dependence of the prefactor on atomistic properties of systems, we have recently developed a calculational scheme[11–13] in which this quantity is evaluated within the validity of transition state theory[14] and the harmonic approximation of lattice dynamics. Our calculated prefactors for adatom self-diffusion on flat and stepped surfaces of Ni(100), Cu(100), and Ag(100) have shown the results to be reasonable and the method to be reliable. The aim in this paper is to extend the technique to a comparative study of the coefficient for vacancy diffusion on these three metal surfaces, as a function of the surface temperature, and thereby evaluate the relative preference for vacancy and adatom diffusion. As in the case of adatoms, we also examine the effects of lateral thermal expansion on activation barriers and prefactors for vacancy diffusion by performing a set of calculations in a restricted quasiharmonic approximation in which we include thermal expansion in the bulk and in the surface plane, but not along the surface normal.

II. THEORETICAL DETAILS

The top view of two essential stages in the diffusion of a monovacancy on a fcc(100) surface are sketched in Fig. 1. At the left of the figure is a minimum-energy configuration in which a monovacancy is shown surrounded by four surface

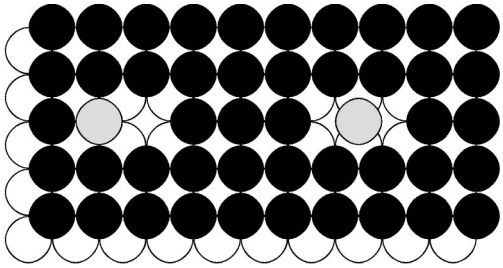

FIG. 1. Top view of fcc(100) surface showing the two steps in monovacancy hopping diffusion. Black circles indicate surface atoms, white circles represent atoms of the second layer. The gray circles represent the tagged surface atom (one of four equivalent atoms for the interchange) in its original (minimum-energy site) position, at left, and in the transition state, at right.

atoms. Vacancy diffusion proceeds when one of these otherwise equivalent atoms jumps towards the vacancy and eventually exchanges its position with the vacancy thereby causing the latter to diffuse. We have shaded such an atom light gray in Fig. 1 and will refer to it as the tagged atom in the rest of the paper. The intermediate stage in this process, shown at the right half of Fig. 1, is the transition state in which the tagged atom is located between its original site and the vacancy. The vacancy moves over the surface by subsequent jumps of neighboring surface atoms into the vacant region. The net result of these jumps is a random walk of the vacancy over the surface.

The diffusion coefficient of an entity performing random walk may be written within the validity of transistion state theory as[13]

$$D = D_0(T)\exp\left(\frac{-\Delta\Phi}{k_B T}\right) \tag{1}$$

with

$$D_0(T) = \frac{k_B T}{h}\frac{nl^2}{2\alpha}\exp\left(\frac{\Delta S_{vib}}{k_B}\right)\exp\left(\frac{-\Delta U_{vib}}{k_B T}\right),$$

where ΔS_{vib}, ΔU_{vib}, and $\Delta\Phi$ are, respectively, the differences in the vibrational entropy, internal energy, and static (structural) energy, for the system with the diffusing entity at the maximum- (saddle point) and the minimum-energy points on the potential-energy surface. These are also called the activation functions. When the diffusing entity is a vacancy, the saddle point refers to the maximum-energy point on the potential-energy surface for the tagged surface atom shown in Fig. 1. Here n is the number of equivalent possibilities for atom-vacancy interchange, l is the jump length, and α is the dimensionality of the process. Note that in the classical limit the equations above are equivalent to those proposed by Vineyard.[15] Our usage of the quantum-mechanical vibrational partition function has interesting consequences for D_0 at low temperatures, as we shall see.

In the harmonic/quasiharmonic approximation of lattice dynamics, the thermodynamical quantities appearing in the above equations assume standard forms that exhibit their dependence on $N(\nu)$, the vibrational density of states as a function of frequency ν. For example,

$$U_{vib} = k_B T\int_0^{\nu_{max}} N(\nu)\left(\frac{1}{2}x + \frac{x}{e^x - 1}\right)d\nu,$$

$$S_{vib} = k_B\int_0^{\nu_{max}} N(\nu)\left[-\ln(1-e^{-x}) + \frac{x}{e^x - 1}\right]d\nu, \tag{2}$$

where $x = h\nu/k_B T$. To examine the contributions from different regions, $N(\nu)$ may be written as $N(\nu) = \Sigma_l n_l(\nu)$, where $n_l(\nu)$ is the local density of states (LDOS) in region l. To calculate the LDOS we solve the secular equation for the force-constant matrix for the entire system and obtain the eigenvalues ν_i and eigenvectors $u_l(\nu_i)$ from which the LDOS at site l in Cartesian direction β is calculated as

$$n_{l,\beta}(\nu) = \sum_i^N \frac{\alpha}{\pi}|u_{l,\beta}(\nu_i)|^2 e^{-\alpha^2(\nu-\nu_i)^2}, \tag{3}$$

where α governs the width of the δ function and the sum runs over all N eigenvalues ν_i.

We shall see that these LDOS depend strikingly on the location of the tagged surface atom along the reaction coordinate (minimum-energy site or in the transition state) and lead to differences in the local thermodynamic functions in these two configurations. The input for calculations of LDOS is the force-constant matrix that we obtain from interaction potentials based on the embedded-atom method[16] (EAM). In our work on adatom self-diffusion, usage has been made of two different sets of EAM potentials: one obtained by Foiles, Baskes, and Daw[16] (FBD) and the other by Voter and Chen[17] (VC). The latter has the advantage that it has been fitted to reproduce correctly the bond strength and bond length of the dimer, in addition to several properties of the bulk metal. Since it is not clear *a priori* which EAM potential is more suitable for examination of monovacancy diffusion on Cu(100), Ag(100), and Ni(100), we use both sets of potentials and judge the extent to which the results depend on specific choice. The procedure for the calculation of the LDOS for the vacancy and tagged atom is very similar to that already described for the adatoms.[12]

The model system consists of 999 atoms arranged in ten layers, such that a missing atom in the surface layer is the vacancy. This system is large enough that finite-size effects can be ignored. Periodic-boundary conditions are applied in the surface (x-y) plane only. Structural total energies are evaluated using a conjugate gradient technique with all atoms relaxed in their minimum energy configuration, in the $3N$-dimensional coordinate space, where N is the number of atoms in the cell. In the transition state, we fix the position of the tagged atom and of the eight edge atoms of the cubic cell, along the reaction coordinate, and carry out the minimization of the total energy in the $3N-9$-dimensional coordinate space. This prevents the tagged atom from returning to the minimum-energy position and the whole crystal from translating along the reaction coordinate. Force-constant matrices for atomic configurations along the diffusion path (minimum energy and transition state) are then calculated from the specific configurations.

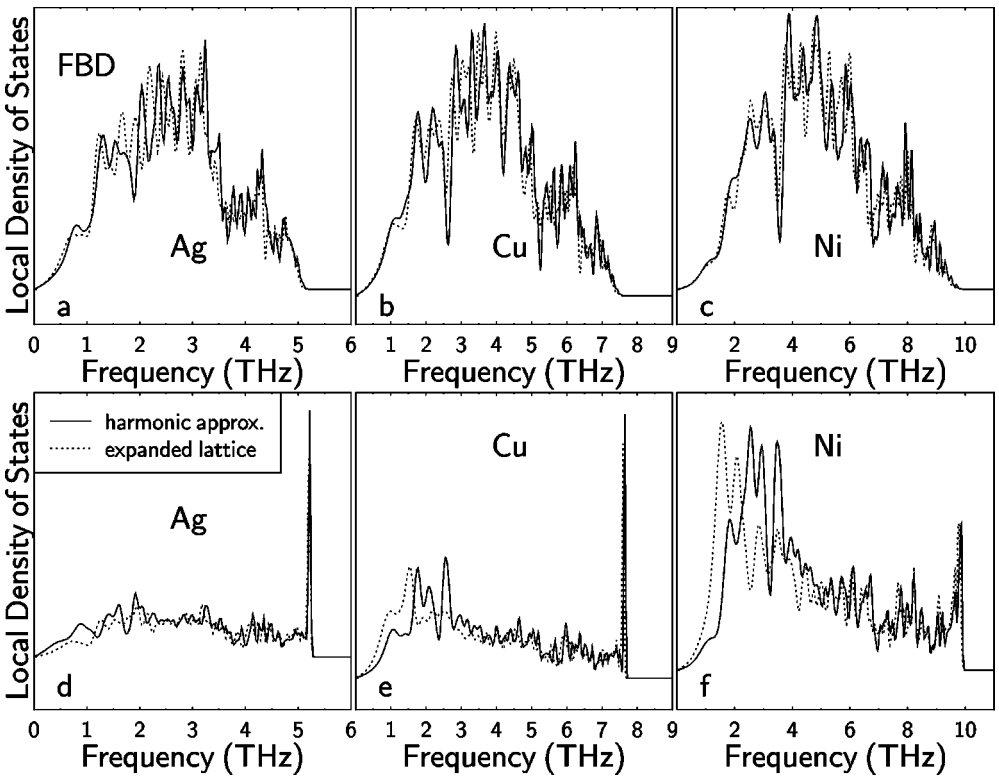

FIG. 2. LDOS for Ag, Cu, and Ni, for the tagged atom in its minimum-energy site [upper row, (a)–(c)] and in the transition state [lower row, (d)–(f)], calculated in the harmonic approximation (solid line) and for an expanded lattice at 600 K (dotted line), using FBD potentials. The values of α were chosen to be $\alpha(\mathrm{Ag})=0.1$, $\alpha(\mathrm{Cu})=0.05$, and $\alpha(\mathrm{Ni})=0.03$.

III. RESULTS AND DISCUSSION

The local vibrational density of states for the tagged atom (and the vacancy) in its minimum-energy site have characteristic appearances regardless of the surface and the potential type, as seen in Figs. 2(a–c) and Figs. 3(a–c). Not surprisingly, these LDOS's resemble those of atoms on fcc (100) surface,[12] since the vacancy is a minor perturbation on the surface. At the same time, a common feature of the LDOS in the transition state, Figs. 2(d–f), and Figs. 3(d–f), is the presence of high-frequency peaks contributed by atomic vibrations along the surface normal (z direction) resulting from a strong bond between the tagged atom and the two atoms in the second layer between which it is located (see Fig. 1). This is analogous to the case for an adatom located in a bridge site (transition state for the hopping process) on a fcc(100) surface, as discussed in earlier works.[11,12] Despite this similarity, the LDOS's for the tagged atom in the transition state exhibit remarkable differences for the three metal surfaces. Each one of these is also strikingly different from the respective one in the panel above it. Interestingly, the LDOS's for the transition state for both Cu(100) and Ni(100) display enhanced contributions at lower frequencies, which are most pronounced in the case of Ni(100) with the FBD potential [Fig. 2(f)]. These features do not appear in the case of Ag(100) and have consequences for its activation entropies and preexponential factors, as we shall see.

We find the qualitative features of the thermodynamic activation functions calculated using the LDOS in Fig. 2 and Fig. 3 to be similar to the corresponding ones for adatom diffusion.[12,13] On each surface the contribution ΔS_{vib} overcompensates that of ΔU_{vib} leading to a net increase in the vibrational free energy (about 100 meV, at 600 K). This increment in Δf_{vib} is smallest for Ni(100) and highest for Ag(100), which can again be traced to the characteristics in the LDOS in Figs. 2 and 3. In the case of Ni(100), the pronounced low-frequency contributions in the LDOS for the tagged atom in the transition state give rise to larger vibrational entropy and smaller differences in the vibrational quantities for the minimum-energy and transition state configurations. Trends in the LDOS also explain the lack of noticeable differences in the thermodynamic functions resulting from the harmonic and the expanded lattice cases. This difference is found to be smallest for Ni(100), understandably because of Ni's significantly higher melting temperature as compared with Cu and Ag. In the same spirit, Δf_{vib} is smaller for the expanded lattice than for the harmonic one for Ni(100) and Cu(100), but not for Ag(100).

The preexponential factors for vacancy diffusion on Ag(100), Cu(100), and Ni(100), calculated with both potentials in the harmonic approximation, are shown as a function of temperature in Fig. 4. The prefactors are largest for Ni(100), followed by Cu(100) and Ag(100), in accordance with the contributions of the respective activation entropies discussed above. The general trends in the three curves show prefactors increasing with temperature until about 200 K beyond which they become almost temperature independent, as expected in the classical limit. The behavior at temperatures below 200 K is reflective of the usage of the quantum-mechanical partition function.

The values for the prefactors (at 600 K) are summarized in Table I. These values are within a factor of 2 of each

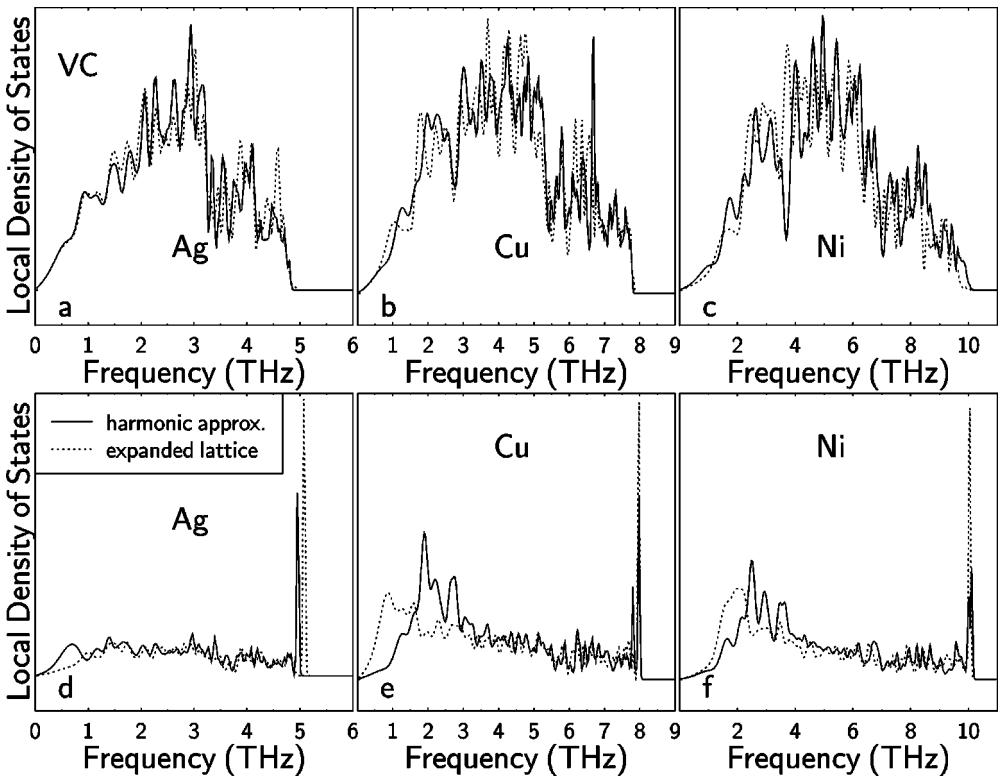

FIG. 3. LDOS for Ag, Cu, and Ni, for the tagged atom in its minimum-energy site [upper row, (a)–(c)] and in the transition state [lower row, (d)–(f)], calculated in the harmonic approximation (solid line) and for an expanded lattice at 600 K (dotted line), using VC potentials.

other. In fact, the values are comparable to those for adatom diffusion on the these surfaces. A quick comparison with Table 2 in Ref. 12 reveals that the prefactors for monovacancy diffusion on Cu(100) are 2.9 (FBD) and 3.6 (VC) times higher than for adatom diffusion. For Ag(100) and Ni(100), the comparison depends more strongly on the form of the interaction potential. The ratio of the prefactors for vacancy and adatom diffusion on Ag(100) are 2.5 (FBD) and 0.9 (VC), while for Ni(100) they are 3.7 (FBD) and 1.1 (VC). Note, that in Ref. 12 the definition of the prefactors did not include ΔU_{vib}, and hence the values need to be multiplied by 2.72 for comparison with those in Table I. Table I also shows that at 600 K the calculation with the expanded lattice gives somewhat higher values of the prefactors for vacancy diffusion on Cu(100) and Ni(100) [lower on Ag(100)], than the one with the 0-K lattice constant. The effects are, however, small and may be ignored as a first approximation.

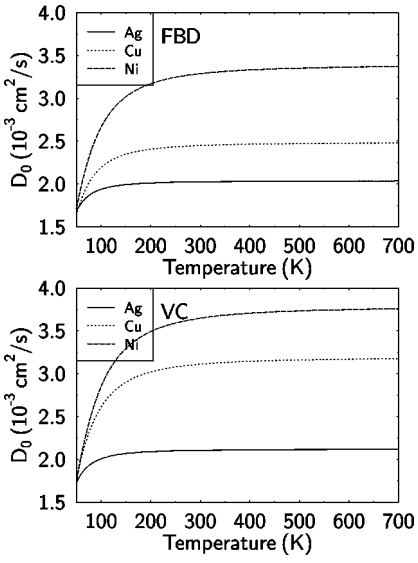

FIG. 4. Temperature dependence of the preexponential factors for vacancy diffusion on Ag(100), Cu(100), and Ni(100), calculated in the harmonic approximation: FBD potential (upper figure), and VC potential (lower figure).

The effect of lateral thermal expansion on activation barriers is documented in Table II in which $\Delta\Phi$ is the barrier calculated with the 0-K lattice constant, and $\Delta\Phi^{quasi}$ is that with lattice constant at 600 K. As the lattice expands laterally, we find a general increase in all barriers. This trend was also observed for adatom hopping on the (100) surfaces of Ag, Ni, and Cu (Refs. 12 and 13) and on Ag(111).[18] Further, a comparison of $\Delta\Phi$ from Table II with the corresponding activation barriers for adatom diffusion (see Ref. 12, Table

TABLE I. Preexponential factors D_0 and D_0^{quasi}, which include contributions from ΔS_{vib} and ΔU_{vib} calculated at 600 K. Here D_0^{quasi} includes lateral thermal expansion of the lattice.

cm^2/s	D_0	D_0^{quasi}
Ag	2.0×10^{-3} (FBD)	1.6×10^{-3} (FBD)
	2.1×10^{-3} (VC)	1.6×10^{-3} (VC)
Cu	2.5×10^{-3} (FBD)	3.0×10^{-3} (FBD)
	3.2×10^{-3} (VC)	4.3×10^{-3} (VC)
Ni	3.4×10^{-3} (FBD)	4.0×10^{-3} (FBD)
	3.8×10^{-3} (VC)	4.0×10^{-3} (VC)

TABLE II. Activation barriers $\Delta\Phi$ and $\Delta\Phi^{quasi}$ calculated with the lattice constant for 0 K and 600 K, respectively.

eV	$\Delta\Phi$	$\Delta\Phi^{quasi}$
Ag	0.47 (FBD)	0.53 (FBD)
	0.45 (VC)	0.50 (VC)
Cu	0.44 (FBD)	0.50 (FBD)
	0.46 (VC)	0.52 (VC)
Ni	0.55 (FBD)	0.67 (FBD)
	0.59 (VC)	0.63 (VC)

1) shows that for Cu(100) and Ni(100) the former are about 13% smaller than the latter, irrespective of the type of EAM potential. In the case of Ag(100), these barriers are of comparable strength [differences: 0.01 eV (FBD) and 0.03 eV (VC) lie within the error margins in EAM].

The above results for prefactors and activation barriers indicate that if adatoms and vacancies are both present on the surface, vacancy diffusion competes quite well with that of adatoms for mass transport. In general, the values of the prefactors and activation barriers for both types of species are comparable, although some differences may be mentioned. Our results indicate that vacancy diffusion may be favored on Cu(100) and Ni(100). For Ag(100) the relative rates for the two processes appear to be similar: FBD potentials give vacancy diffusion an edge, while VC potentials yield quite comparable rates for the two. Given the limits of accuracy of empirical potentials like the EAM, however, it is best to emphasize here the qualitative similarities rather than the small differences in the magnitudes of various diffusion coefficients that we have calculated. It should also be remembered that in reaching these conclusions about preferences for vacancy or adatom surface diffusion we have not taken into account the respective formation energies, since our aim was to compare only their migration rates. In making connection with specific experiments, it would be important to know more details like sample preparation technique, and the presence of islands, steps, or kinks, as the availability of adatoms and vacancies on surfaces may depend on them. Both species may also be created as vacancy-adatom pairs[19] yielding the same amounts of each.

Of the three surfaces studied here, Cu(100) has been the subject of most intense discussion vis-a-vis the preference for vacancy diffusion in mass transport. It is proposed to be the dominant mechanism in previous theoretical calculations[3,9] and analysis of experimental data[10]. Our results suggest that vacancies compete well with adatoms in surface migration on Cu(100). Whether or not they are favored over adatoms depends on the relative concentration of vacancies and adatoms at a specific temperature. It should be pointed that our calculated preexponential factors for vacancy diffusion are smaller than those obtained in recent molecular dynamics simulations.[9] This is not surprising, since the simulations were performed in a temperature range of 650 K to 980 K. At these high temperatures enhanced anharmonicity plays an important role[20–22] with consequences for prefactors, as demonstrated by Suni and Seebaur[2].

IV. SUMMARY

We have calculated activation barriers and preexponential factors for monovacancy diffusion on Ag(100), Cu(100), and Ni(100) surfaces, by including explicitly the contribution of the activation vibrational free energy, which was calculated from the local vibrational density of states of the tagged atom in its two relevant positions (minimum energy and transition state). The results for the three metal surfaces show that the vibrational entropy contributions, and hence the prefactors, depend on particular features of the LDOS. We find that at temperatures beyond 200 K diffusion prefactors become almost constant. Below 200 K they decrease with decreasing temperature to vanish at 0 K, as a consequence of the usage of the quantum-mechanical partition function. In general we find the differences in the results obtained from the harmonic approximation and from that for the expanded lattice to be small. The most noticeable impact of the expanded lattice calculations is on the activation barriers that increase with lattice expansion for all three metal surfaces and independent of the potential type. Although the quantitative details may depend on the details of the interaction potential, we find for all three surfaces the diffusion coefficients for monovacancies to be comparable to that of adatoms, if not larger. Thus in consideration of mass transport on surfaces, the role of vacancies cannot be ignored. These results await verification by further experimental data and more sophisticated theoretical calculations.

[1] J. B. Adams, S. M. Foiles, and M. G. Wolfer, J. Mater. Res. **4**, 102 (1989); M. Nomura, S.-Y. Lee, and J. B. Adams, *ibid.* **6**, 1 (1990); C.-L. Liu and S. J. Plimpton, Phys. Rev. B **51**, 4523 (1995); S. B. Debiaggi, P. M. Decorte, and A. M. Monti, Phys. Status Solidi B **195**, 37 (1996).

[2] I. I. Suni and E. G. Seebauer, Surf. Sci. Lett. **301**, L235 (1994).

[3] M. Karimi, T. Tomkowski, G. Vidali, and O. Biham, Phys. Rev. B **52**, 5364 (1995).

[4] C. L. Liu and J. B. Adams, Surf. Sci. **265**, 262 (1992).

[5] P. Wynblatt and N. A. Gjostein, Surf. Sci. **12**, 109 (1968).

[6] B. Perraillon, I. M. Torrens, and V. Levy, Scr. Metall. **6**, 611 (1970).

[7] G. Delorenzi and G. Jacucci, Surf. Sci. **116**, 391 (1982).

[8] A. F. Voter, Proc. SPIE **821**, 214 (1987).

[9] G. Boisvert and L. J. Lewis, Phys. Rev. B **56**, 7643 (1997).

[10] J. B. Hannon, C. Klünker, M. Giesen, H. Ibach, N. C. Bartelt, and J. C. Hamilton, Phys. Rev. Lett. **79**, 2506 (1997).

[11] U. Kürpick, A. Kara, and T. S. Rahman, Phys. Rev. Lett. **78**, 1086 (1997).

[12] U. Kürpick and T. S. Rahman, Surf. Sci. **383**, 137 (1997).

[13] U. Kürpick and T. S. Rahman, Phys. Rev. B **578**, 2482 (1998).

[14] S. Glasstone, K. J. Laidler, and H. Eyring, *The Theory of Rate Processes* (McGraw-Hill, New York, 1941).

[15] G. H. Vineyard, J. Phys. Chem. Solids **3**, 121 (1957).

[16] S. M. Foiles, M. I. Baskes, and M. S. Daw, Phys. Rev. B **33**, 7983 (1986).

[17] A. F. Voter and S. P. Chen, in *Characterization of Defects in Materials*, edited by R. W. Siegel, J. R. Weertman, and R. Sinclair, MRS Symposia Proceedings No. 82 (Materials Research Society, Pittsburgh, 1986), p. 175.
[18] C. Ratsch, A. P. Seitsonen, and M. Scheffler, Phys. Rev. B **55**, 6750 (1997).
[19] P. Stolze, J. Phys.: Condens. Matter **6**, 9495 (1994).
[20] L. Yang. T. S. Rahman, and M. S. Daw, Phys. Rev. B **44**, 13 725 (1991).
[21] L. Yang and T. S. Rahman, Phys. Rev. Lett. **67**, 2327 (1991).
[22] G. Bracco, L. Bruschi, L. Pedemonte, and R. Tatarek, Surf. Sci. **352-354**, 964 (1996).